IET Electric Power Applications

Research Article

IET Journals
The Institution of Engineering and Technology

Proposed diagnostic methodology using the cross-correlation coefficient factor technique for power transformer fault identification

ISSN 1751-8660
Received on 12th August 2016
Revised on 6th December 2016
Accepted on 14th December 2016
doi: 10.1049/iet-epa.2016.0545
www.ietdl.org

Saber M. Saleh[1] ✉, *Salah Hamdy EL-Hoshy*[2], *Osama E. Gouda*[3]

[1]*Department of Electrical Power and Machines, Faculty of Engineering, Fayoum University, Al Fayoum, Egypt*
[2]*Middle Egypt Electricity Zone, Egyptian Electricity Transmission Company, El-Fayoum, Egypt*
[3]*Department of Electrical Power and Machines, Faculty of Engineering, Cairo University, Cairo, Egypt*
✉ *E-mail: sabermssh@gmail.com*

Abstract: This study investigates the impact of electrical parameter variation of a high-frequency transformer model on its sweep frequency response analysis (SFRA) signature to help in classification and interpretation. The simulations have been done using MATLAB and compared with the reference data. The results of SFRA measurements are repeatable up to and beyond 1MHz. The proposed diagnostic methodology using the Cross-Correlation Coefficient Factor (CCF) is used to identify the transformer faults. CCF used to measure the degree of relationship between two variables that establish a relation between the predicted and actual data set. The results of this proposed methodology using the CCF compared with existing Chinese Standard factor (CSF) indicate that, the proposed method is valid to identify the transformer faults. Characteristics of the proposed scheme are fully analyzed by extensive MATLAB simulation studies that clearly reveal that this method can accurately identify the transformer faults compared with CSF. And also does not affected by different fault conditions such as transformer normal condition, Turn to Turn Fault for both HV, LV sides, Axial Fault and/or Radial Faults on both sides, Short Circuit Fault between H.V and L.V Sides, Short Circuit to Ground Fault for both HV, LV sides.

1 Introduction

Transformer insulation deteriorates as the function of temperature, moisture and time. The core and winding losses, stray losses in a tank and metal support structures are the principle sources of heat which cause oil and winding temperature rise. There are multiple reasons for overheating, such as improper cooling, excessive eddy currents, bad joints, blocked radiators, overloading, improper earthing and harmonic contents in the power supply. This leads to accelerated aging of oil and cellulosic solid insulation, which generate the gasses within the transformer and further leads to permanent failure. To prevent such failures, effective analysis, and diagnosis needs to be investigated [1].

The sweep frequency response analysis (SFRA) is a proactive technique which is used to detect mechanical faults in transformers. Distortions in the transformer windings can be the result of forces due to high short-circuit (SC) current, damage during transportation and installation and so on [2]. It is based on the principles that change in windings as a result of deformation and displacements corresponding to modification in the impedance of the transformer and accordingly results in alteration of its frequency response spectrum [3]. This technique utilises a sweep generator to apply sinusoidal voltages at different frequencies to one terminal of the transformer. The output amplitude and phase signals from selected terminals of the transformer can then be plotted as a function of frequency. If there are any mechanical changes in the transformer, for example, the windings are moved or distorted; its fingerprint will also be changed so theoretically, the mechanical changes in the transformer can be detected with the SFRA. This definition is consistent with the SFRA method used by proposing diagnostic methodology using the cross-correlation coefficient factor (CCF) technique.

Several researchers in recent years have presented many techniques aimed at power transformer fault identification. Table 1 summarises the comparison between the proposed method and the recent researches.

2 Transfer function

A transfer function is defined as a mathematical representation of the relation between the input and output signals. The input and output signals give the transfer functions its physical interpretation, for example, if the output is a voltage and the input is current, then the transfer function will be impedance. For the transfer function, there will be a magnitude and phase which both varies with frequency and which can be measured experimentally [12].

2.1 Frequency response measurements

SFRA proceeds by injecting a sinusoidal voltage signal of constant amplitude with variable frequency to one end of the transformer winding and the output signal is measured from the other end of the winding as shown in Fig. 1 [12]. The transfer function results from a comparison of the input and output signals.

The frequency response is calculated as the ratio of the transmitted voltage waveform (V_{out}) to the applied voltage waveform (V_{in}) in dB using the following equation [13]

$$\text{Magnitude response (dB)} = 20\text{Log}_{10}\left(\frac{\text{Output voltage}}{\text{Input voltage}}\right) \quad (1)$$

$$\text{Phase response}(^\circ) = \tan^{-1}\left(\frac{\text{Output voltage}}{\text{Input voltage}}\right) \quad (2)$$

Based on a resulting set of SFRA traces (mainly the amplitude in dB shown over the frequency) an evaluation of the transformer's mechanical condition is commonly based on frequency spectrum comparison [14]. There are mainly three strategies are commonly used to assess the measured traces:

- Time-based (current SFRA results will be compared with previous results of the same unit).

Table 1 Comparison between the proposed method and the recent researches

Ref.	Title	The main difference
	Proposed diagnostic methodology using the CCF technique for power transformer fault identification	• The simulated responses are studied for a turn-to-turn fault in power transformer for both high-voltage (HV) and low-voltage (LV) sides, electromechanical forces of transformer windings included axial fault, radial faults on both sides, SC fault between HV and LV sides, SC-to-ground fault for both HV and LV sides based on normal condition. • The simulated responses are studied by subdividing into three frequency regions and compared using the correlation coefficient to estimate faulted components which caused the deviation in the response. • The simulated responses are studied by subdividing into three frequency regions and compared using Chinese Standard DL/T 911 – 2004 technique to evaluate to estimate faulted components which caused the deviation in the response. • Making a comparison between the Chinese Standard factor (CSF), CCF technique in order to evaluate the optimum location of mechanical and electrical stresses of power transformer. • The suggested correlation coefficient (same phase) limits as four limits for each region. ○ Normal 0.90–1.0 ○ Slight deformation 0.70–0.90 ○ Obvious deformation 0.30–0.70 ○ Serious deformation <0.3
[4]	Study of transformer winding deformation by frequency response analysis	• The simulated responses are studied for inter-turn, inter-disc and inter-winding capacitances of the winding based on normal condition. So, suitable for inter-turn fault only. • The simulated responses are studied by subdividing into four frequency regions and compared using the correlation coefficient to estimate faulted components which caused the deviation in the response. Four regions need more computation time and slower than our proposed. • From the Nyquist diagram, it was observed that the real minimum of each plot increases as the winding deformation increases to analyse the shape of each plot. The phase against frequency graph does not contain as much useful information as the amplitude against frequency graph does, due to the influence of noise in the output signal results and the result of the SFRA measurement.
[5]	A new technique for a better sweep frequency response analysis interpretation	• Evaluate the cross-correlation coefficient of the computed time–frequency distribution. General curve probabilistic, not deterministic. • It does not give data which show the fault location.
[6]	Using cross-correlation coefficients to analyse transformer SFRA traces	• The simulated responses are studied by subdividing into four frequency regions and compared using the correlation coefficient to estimate faulted components which caused the deviation in the response. • Sister unit (same phase) limits as three limits for each region. ○ Good 0.95–1.0 ○ Marginal 0.90–0.94 ○ Investigate <0.90 Margin is inherent with respect to the actual case.
[7]	Artificial neural network and cross-correlation based features for discrimination between electrical and mechanical defects and their localisation in transformer winding	• The simulated responses are studied for disc-to-disc SC faults, radial deformation and axial displacement defects based on normal condition. • It does not give data which show the fault location. • All cases not covered • General curve
[8]	Statistical evaluation of a new technique for SFRA	• Evaluate the cross-correlation coefficient of the computed time–frequency distribution. • It does not give data which show the fault location. • General curve probabilistic, not deterministic.
[9]	Diagnosing transformer faults using frequency response analysis	• The simulated responses are studied by subdividing into five frequency regions and compared using the correlation coefficient to estimate faulted components which caused the deviation in the response. • The reference limit unknown.
[10]	Robust transfer function identification via an enhanced magnitude vector fitting (VF) algorithm	• In this paper, VF is a numerical method for rational approximation in the frequency domain using poles and residues. However, a robust procedure is presented to identify a complex transfer function of a linear time-invariant system from magnitude data. In this approach, building a rational modelling from magnitude square frequency responses, followed by spectral factorisation. Then, discarding poles and zeros located in the right half-plane to recover a minimum phase shift magnitude approximation. Finally, determine a minimum-phase rational function whose magnitude approximates the given magnitude response. • It's an enhanced version of the VF algorithm which used to identify high-frequency models of transformers based on its magnitude frequency response. It does not give data which show the fault identification. This technique can be used to identify diagnosis fault of power transformer and overhead transmission line.
[11]	Investigation of the transformer winding high frequency parameters identification using particle swarm optimisation (PSO) method	In this paper, using PSO method to identify the parameters of the transformer winding for diagnostic purposes and compared with transfer function and genetic algorithm methods. Step 1: Create the random initial swarm each particle swarm contains the values of the mutual and self-inductances and also the values of the ground capacitance and shunt capacitance per each section as A and B population. Step 2: Evaluate fitness function for each particle; each particle swarm is put at the initial set referring to the value of the fitness function. Step 3: Check and update personal best and global best; the algorithm parameters are determined as follows: the P-best is the best position of each particle so far and the G-best is the best position of all generations. Then, compare particle fitness evaluation with particle P-best and also compare fitness evaluation with the population overall previous best. Step 4: Estimating the open circuit and SC of natural frequencies using the matrices ***L***, ***C*** and ***R***. Step 5: The PSO algorithm stops when the criteria are successes. So, this method detects the fault but not identify the type.

• Type-based (SFRA of one transformer will be compared with another of the same design).
• Phase comparison (SFRA results of one phase will be compared with the results of the other phases of the same transformer).

3 Power transformer model

MATLAB software is used to simulate the transformer model shown in Fig. 2 [15]. The model includes distributed inductance and resistance, mutual inductance, and three capacitances including, inter-winding, self, and ground capacitance. In the model under study, the high voltage (*HV*) and low voltage (*LV*) windings are assumed to consist of 15 disks each that comprise 140 and 15 turns, respectively. Each disk comprises the following parameters are in their lumped form: series resistance (R_s) and inductance (L_s) shunted by a capacitor (C_{sh}), and a conductance (G_{sh}). The capacitance between *HV* and *LV* windings (C_{HL}) is shunted by dielectric conductance (G_{HL}), also, mutual inductances (M_{ij})

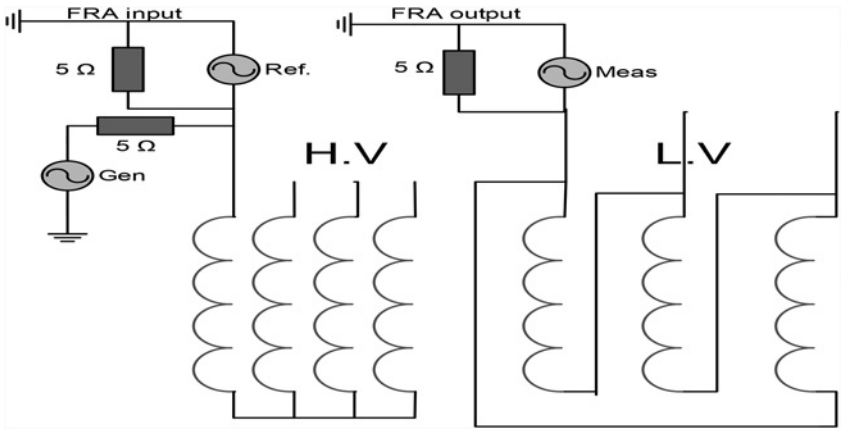

Fig. 1 *Frequency response analysis measurement*

between relevant coils are represented. The dielectric insulation between the *LV* winding and the earthed core and that is between the *HV* winding and the earthed tank is simulated by a capacitance (C_g) and dielectric conductance (G) as shown in Fig. 2. The physical meaning of the model parameters allows the identification of the problem inside the transformer and helps in establishing a standard code for SFRA signature interpretation. There is a model for step-down power transformer two-winding with a regulating winding connecting the *HV*-winding to the neutral is developed. Hints, capacitance from the leads, tap-changer, static-plates, and

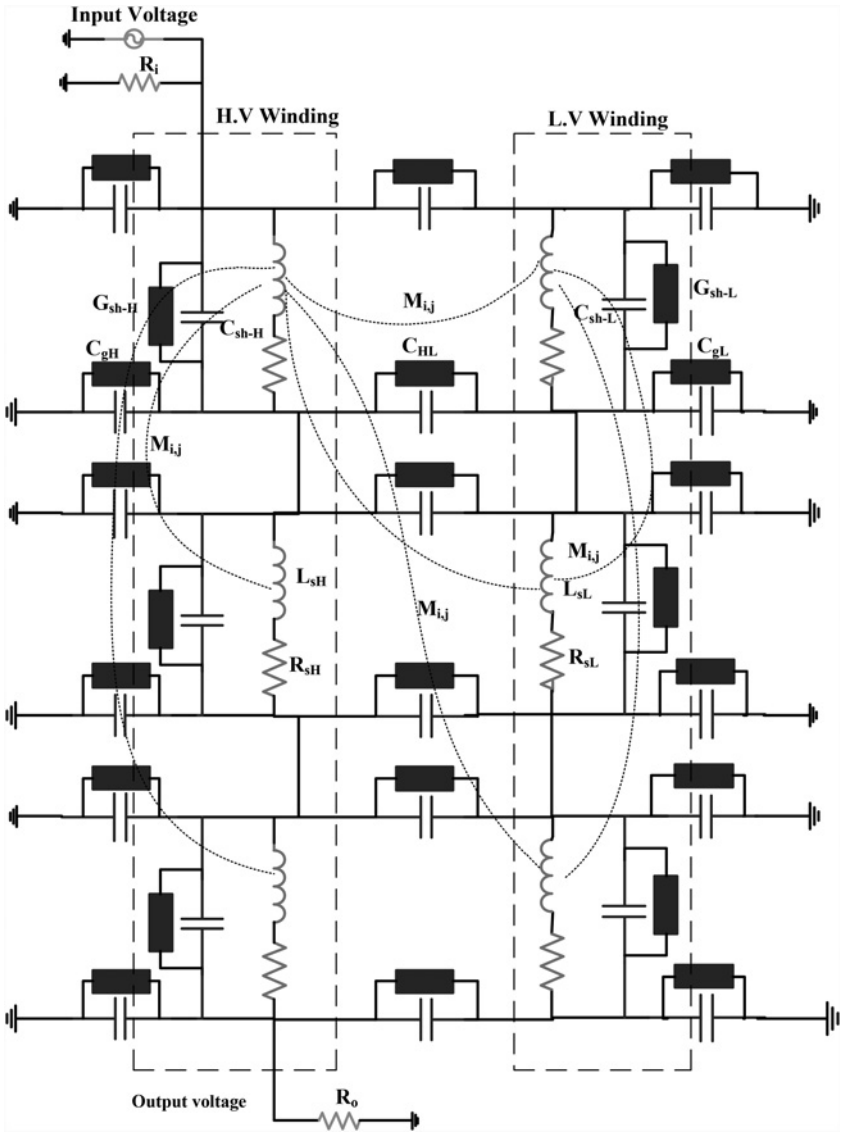

Fig. 2 *High frequency transformer model and winding geometry*

IET Electr. Power Appl., 2017, Vol. 11, Iss. 3, pp. 412–422

Table 2 Electrical parameters of the transformer linear model

	R_S, Ω	L_S, μH	C_{SH}, nF	C_g, pF	C_{HL}, nF	1/G, MΩ
HV	1.2	145	2.20	37	3.53	7
LV	0.75	110	0.2	6	3	7

shields are implemented on an empirical basis. Bushing capacitance is added as lumped capacitance on the terminals. The following nameplate information is given [16]

HV:60 kV $\pm$ 6 × 1.46% (Reg.winding), 20 MVA, 195 A, *YN*

LV:6, 6 kV, 20 MVA, 1724 A, *yn*0

The measured values of the above parameters are listed in Table 2 [16].

During the investigation, a voltage signal is applied to the high-frequency transformer model and using MATLAB, the generated output for a wide frequency range is plotted with logarithmic amplitude in decibels against the frequency to present the analysis.

The authors recognise that such a modelling is subject to some assumptions and may be errors due to neglecting of the changes in model parameters especially the change in capacitors, inductances and even the model resistances of faulty phases [17]. Unfortunately these parameters of the damaged phases are difficult to be calculated.

4 Proposed diagnostic methodology using the CCF technique

Cross-correlation coefficient is a measure of the degree of relationship between two variables which helps in establishing a relation between the predicted and actual data set. The correlation coefficient may take on any value between −1.00 and +1.00.

$$-1.00 \geq R \leq +1.00 \tag{3}$$

A perfect negative correlation is represented by the value −1.00, while a 0.00 indicates no correlation and a +1.00 indicates a perfect positive correlation.

- *Positive correlation:* is where the two variables react in the same way, increasing or decreasing together (high values of $X(i)$ associated with high values of $Y(i)$).
- *Negative correlation:* as one variable increases, the other decreases (high values of $X(i)$ associated with low values of $Y(i)$).
- *No correlation:* there is no relationship between the two variables such that the value of one variable change and the other variable remain constant is called no or zero correlation (values of $X(i)$ are not at all predictive of the values of $Y(i)$).

To calculate a cross-correlation coefficient, there are three different sums of squares (SS). The sum of squares for variable $X(i)$, the sum of square for variable Y, and the sum of the cross-product of $X(i)Y(i)$. Let's say we have a two-transfer function amplitude sequence, each with a length of n: $X(i)$, $Y(i)$, $i = 0, 1, \ldots, n-1$ and $X(i)$, $Y(i)$ are different combinations of real data sets then, the CCF can be calculated and an assessment of the transformer condition can be made as follows [4]

(i) Calculate the sum of squares for variable $X(i)$

$$\mathrm{SS}_{XX} = \sum_{i}^{n} (X_i - \bar{X})^2 \tag{4}$$

(ii) Calculate the sum of squares for variable $Y(i)$

$$\mathrm{SS}_{YY} = \sum_{i}^{n} (Y_i - \bar{Y})^2 \tag{5}$$

Table 3 Cross-correlation coefficients factor and degree of deformation of power transformer

Cross-correlation coefficients factor	Degree of deformation of power transformer
CCF > 0.95	normal deformation of power transformer
0.7 < CCF ≤ 0.95	slight deformation of power transformer
0.3 < CCF ≤ 0.7	obvious deformation of power transformer
CCF ≤ 0.3	severe deformation of power transformer

(iii) Calculate the sum of the cross-products (SS_{XY})

$$\mathrm{SS}_{XY} = \sum_{i}^{n} (X_i - \bar{X})(Y_i - \bar{Y}) \tag{6}$$

where Y_i, $\bar{Y}$ are the original data values and the mean of the original data values and modelled values, respectively.

(iv) Calculate cross-correlation coefficients meeting the project requirements as per the following formula

$$\mathrm{CCF} = \frac{\mathrm{SS}_{XY}}{\sqrt{(\mathrm{SS}_{XX})} * \sqrt{(\mathrm{SS}_{YY})}} \tag{7}$$

(v) To classify the degree of deformation of power transformer as shown in Table 3.

5 Proposed method results and discussion

The proposed method is verified by test the transformer internal faults as compared with health transformer. The cases include normal condition, turn-to-turn fault in power transformer for both HV and LV sides, electromechanical forces of transformer windings included axial fault, radial faults on both sides, SC fault between HV and LV sides, SC-to-ground fault for both HV and LV sides [18–24]. To evaluate the proposed diagnostic methodology using the CCF technique compared with chaise standard factor technique also included.

5.1 Normal condition

Fig. 3 shows the normal condition, response when the power transformer is healthy. The used model for transformer testing is given in Fig. 2 and the data for the tested transformer are given in Table 2. The response curves are done by simulating power transformer without making any fault. It shows a typical response from 10 Hz to 1 MHz, a plot of admittance magnitude versus frequency at normal condition within power transformer. The frequency normally is presented in logarithmic scale and the magnitude is usually shown in decibels. A linear scale for the frequency and the magnitude are used occasionally as well. There are many points of frequency which represent the resonance point (peak of the curve) and anti-resonance point. The number of resonances depends upon a number of turns of each disk of the power transformer. The number of resonance and anti-resonance frequencies increase as the number of disks increases.

The first resonance is occurring at 350 Hz. Beyond this resonance point, the inductance of the transformer winding dominates. While, after the first resonance point the magnetic effect of the winding is trying to increase but winding inductance effect screened. This process continuously repeats several times, so that the medium frequency range has a number of resonance points. After medium frequency range, the winding inductance effect is completely cancelled due to the series and shunt capacitance of the windings as shown in Fig. 3.

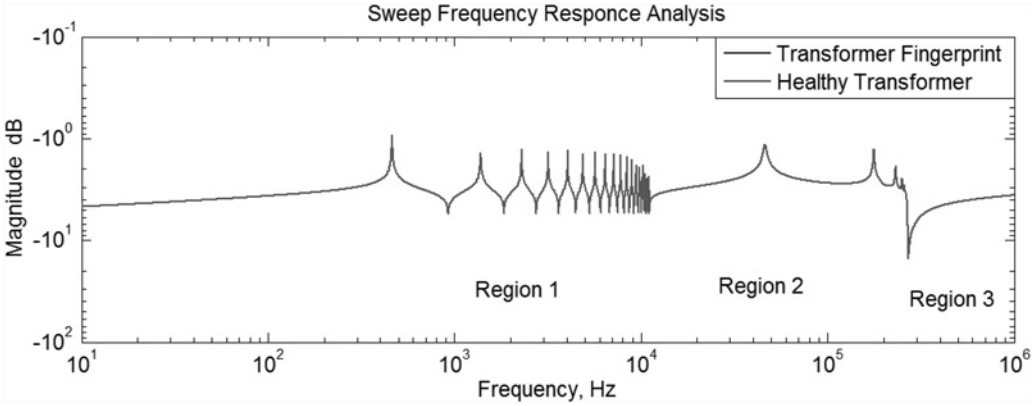

Fig. 3 *Power transformer test at normal condition*

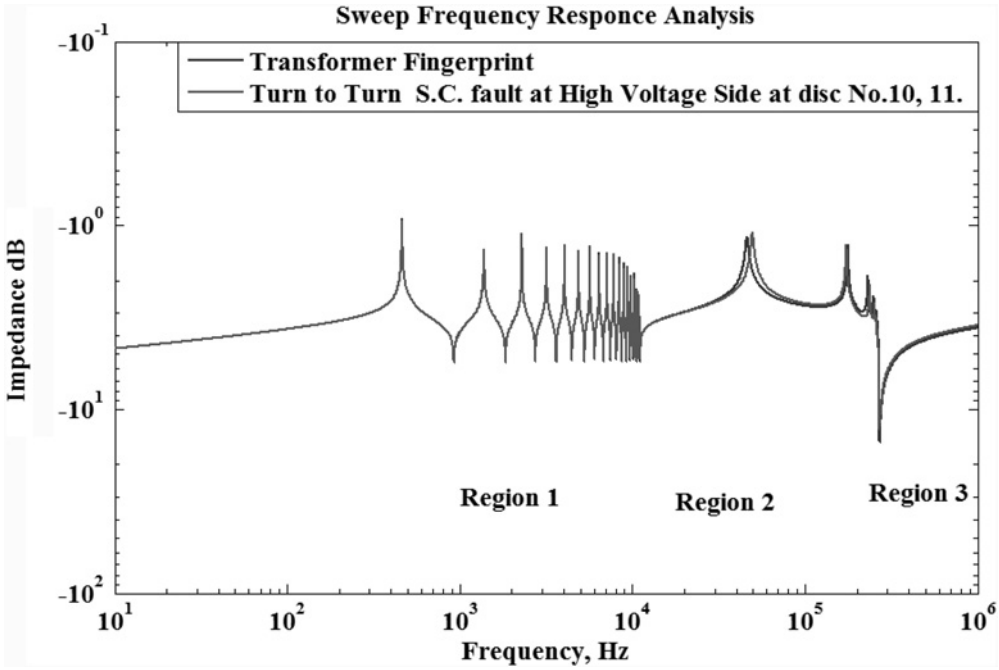

Fig. 4 *SFRA of power transformer at turn-to-turn SC at HV side*

5.2 Turn-to-turn fault in power transformer

A turn-to-turn faults are the most common of insulation type failures. When a SC of a few turns of the transformer winding occurs, it will give rise to a heavy fault current in the short-circuited turns due to the low impedances between those turns. These winding faults produce degradation of the insulation system due to thermal, electrical, and mechanical stress. This degradation leads to reduced insulation quality, which will eventually cause a breakdown in the insulation; either lead to adjacent winding turns being shorted (turn-to-turn SC fault), or directly to a winding being shorted to the ground (winding to ground failure). Based on the above reasoning, sweep frequency response analysis is used to detect such winding turn-to-turn faults before they develop into more serious and costly to repair. The SERA of turn-to-turn SC at HV side at disc number 10, 11 are shown in Fig. 4.

5.2.1 Turn-to-turn SC fault at HV side: At HV side, this fault is simulated by changing (C_{sh} from 2.2 to 32.2 nF), (C_{gH} from 37 to 57 pF), and (R_{SH} from 1.2 to 0 Ω). The short simulation is done between disk no. 10-11, in order to attain variation on a frequency response curve. For the investigation, based on analysing the above traces in different frequency bands, the diagnostic methodology using the CCF attempts have been made at creating automated SFRA analysis tools based on dividing the response into three zones as shown in Table 4.

5.2.2 Turn-to-turn SC fault at LV side: At LV side, this fault is simulated changing (C_{sL} from 0.2 to 32.2 nF), (C_{gL} from 6 to 26 pF), and (R_{SL} from 0.75 to 0 Ω). The short simulation is done between disk no. 10-11, in order to attain variation on a frequency response curve. The proposed algorithm result is shown in Table 5.

5.2.3 Turn-to-turn open-circuit (OC) fault at HV side: At HV side, this fault is simulated by changing, (C_{sH} from 2.2 nF to OC), (C_{gH} from 37 to 57 pF), and (R_{SH} from 1.2 Ω to OC). It will become an OC at the HV side between disk no. 10-11. The diagnostic methodology using the CCF technique indicators according to three frequency sub-bands are given in Table 6.

5.2.4 Turn-to-turn OC fault at LV side: At LV side, this fault is simulated by changing, (C_{sH} from 2.2 nF to OC), (C_{gH} from 6 to 26 pF), and (R_{SH} from 0.75 Ω to OC). It will become an OC at LV side between disk no. 10-11. The proposed technique indicators according to three frequency sub-bands are given in Table 7.

IET Electr. Power Appl., 2017, Vol. 11, Iss. 3, pp. 412–422

Table 4 Transformer state and comparison of using CCF and CSF techniques at HV turn to turn SC fault

Analysis factors	Methods	Frequency ranges						Final action for each method
		Low frequency		Medium frequency		High frequency		
		Frequency < 100 kHz		100–600 kHz		Frequency > 600 kHz		
		Ref.	Faulted	Ref.	Faulted	Ref.	Faulted	
CCF	proposed using CCF technique	1.0000	0.7493	1.0000	0.5236	1.0000	1.0000	obvious deformation and maintenance must be started
action suggestion		slight deformation must be under surveillance		obvious deformation maintenance must be started		no fault		
variance	previous CSF technique	4.7331×10^{-5}	5.3598×10^{-5}	2.0350×10^{-5}	2.1496×10^{-5}	1.7430×10^{-9}	2.8073×10^{-9}	slight deformation and must be under surveillance
NCF		1.0000	0.7493	1.0000	0.5236	1.0000	1.0000	
relative factors		10	1.3834	10	0.7416	10	17.4883	
action suggestion		slight deformation must be under surveillance		slight deformation must be under surveillance		no fault		
transformer case is		slight deformation and transformer must be under surveillance						

Table 5 Transformer state and comparison of using CCF and CSF techniques at low voltage turn to turn S.C fault

Analysis factors	Methods	Frequency ranges						Final action for each method
		Low frequency		Medium frequency		High frequency		
		Frequency < 100 kHz		100–600 kHz		Frequency > 600 kHz		
		Ref.	Faulted	Ref.	Faulted	Ref.	Faulted	
CCF	using CCF technique	1.0000	0.5505	1.0000	0.4090	1.0000	1.0000	obvious deformation and maintenance must be started
action suggestion		obvious deformation maintenance must be started		obvious deformation maintenance must be started		no fault		
variance	previous CSF technique	4.7331×10^{-5}	4.8273×10^{-5}	2.0350×10^{-5}	1.2344×10^{-5}	1.7430×10^{-9}	2.4786×10^{-9}	obvious deformation and maintenance must be started
NCF		1.0000	0.5505	1.0000	0.4090	1.0000	1.0000	
relative factors		10	0.7997	10	0.5260	10	16.7416	
action suggestion		obvious deformation maintenance must be started		obvious deformation maintenance must be started		no fault		
transformer case is		obvious deformation and the transformer maintenance must be started						

Table 6 Transformer state and comparison of using CCF and CSF techniques at HV turn to turn OC fault

Analysis factors	Methods	Frequency ranges						Final action for each method
		Low frequency		Medium frequency		High frequency		
		Frequency < 100 kHz		100–600 kHz		Frequency > 600 kHz		
		Ref.	Faulted	Ref.	Faulted	Ref.	Faulted	
CCF	using CCF technique	1.0000	0.0986	1.0000	0.4524	1.0000	1.0000	serious deformation and transformer must be replaced
action suggestion		serious deformation transformer must be replaced		obvious deformation maintenance must be started		no fault		
variance	previous CSF technique	4.7331×10^{-5}	1.1380×10^{-5}	2.0350×10^{-5}	3.7802×10^{-5}	1.7430×10^{-9}	3.7165×10^{-10}	serious deformation and transformer must be replaced
NCF		1.0000	0.0986	1.0000	0.4524	1.0000	1.0000	
relative factors		10	0.1038	10	0.6022	10	13.6162	
action suggestion		serious deformation transformer must be replaced		slight deformation must be under surveillance		no fault		
transformer case is		serious deformation and must be replaced						

5.3 Electromechanical forces of transformer windings

5.3.1 Axial fault: In this case, the fault can be simulated by changing (R_{SH} from 1.2 to 0.75 Ω), (L_{SH} from 145 to 200 μH), (C_{HL} from 3.3 to 13.3 nF), (R_{SL} from 0.75 to 0.5 Ω), and (L_{SH} from 110 to 150 mH). The SFRA response is shown in Fig. 5 and the proposed method using CCF algorithm result based on dividing the response into three zones as shown in Table 8.

5.3.2 Radial fault at HV side: At HV side, this fault is simulated by changing (R_{SH} from 1.2 to 0 Ω), (L_{SH} from 145 μH to 0.0 H), (C_{HL} from 3.3 to 13.3 nF), (C_{SH} from 2.2 to 12.2 nF), and (C_{gH}

Table 7 Transformer state and comparison of using CCF and CSF techniques at LV turn to turn OC fault

Analysis factors	Methods	Frequency ranges						Final action for each method
		Low frequency		Medium frequency		High frequency		
		Frequency < 100 kHz		100–600 kHz		Frequency > 600 kHz		
		Ref.	Faulted	Ref.	Faulted	Ref.	Faulted	
CCF	using CCF technique	1.0000	0.5799	1.0000	0.9982	1.0000	1.0000	obvious deformation and maintenance must be started
action suggestion		obvious deformation maintenance must be started		no fault		no fault		
variance	previous CSF technique	4.7331×10^{-5}	4.3282×10^{-5}	2.0350×10^{-5}	2.0348×10^{-5}	1.7430×10^{-9}	1.7134×10^{-9}	obvious deformation and maintenance must be started
NCF		1.0000	0.5799	1.0000	0.9982	1.0000	1.0000	
relative factors		10	0.8672	10	6.2944	10	22.6889	
action suggestion		obvious deformation maintenance must be started		no fault		no fault		
transformer case is		deformation and transformer maintenance must be started						

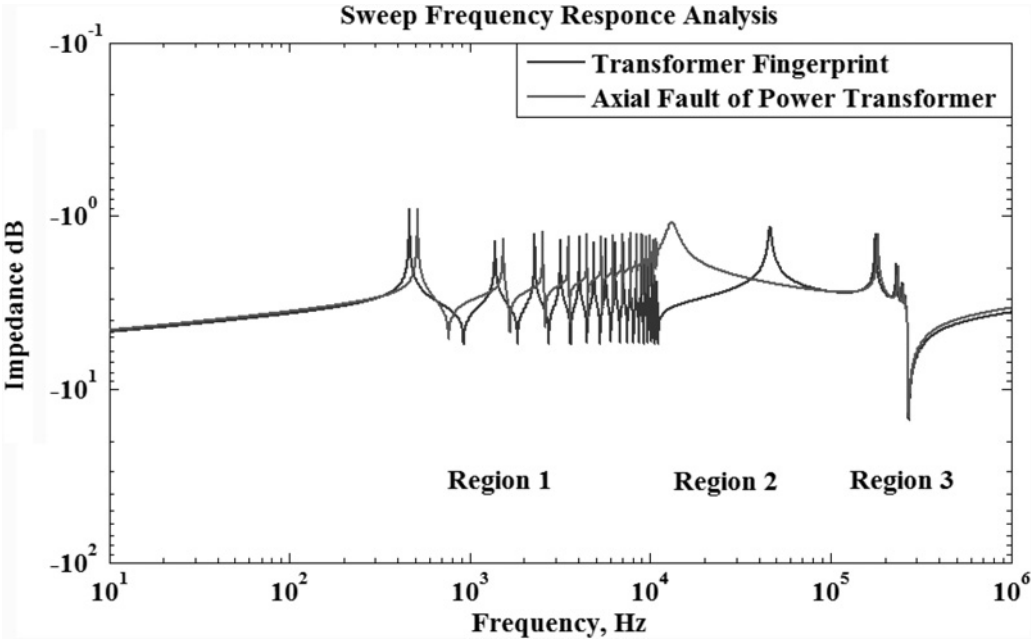

Fig. 5 *SFRA of power transformer at axial fault*

Table 8 Transformer state and comparison of using CCF and CSF techniques at axial fault

Analysis factors	Methods	Frequency ranges						Final action for each method
		Low frequency		Medium frequency		High frequency		
		Frequency < 100 kHz		100–600 kHz		Frequency > 600 kHz		
		Ref.	Faulted	Ref.	Faulted	Ref.	Faulted	
CCF	using CCF technique	1.0000	−0.0204	1.0000	0.4008	1.0000	1.0000	serious deformation and transformer must be replaced
action suggestion		serious deformation transformer must be replaced		obvious deformation maintenance must be started		no fault		
variance	previous CSF technique	4.7331×10^{-5}	1.4429×10^{-4}	2.0350×10^{-5}	2.0894×10^{-5}	1.7430×10^{-9}	4.4378×10^{-9}	serious deformation and transformer must be replaced
NCF		1.0000	−0.0204	1.0000	0.4008	1.0000	1.0000	
relative factors		10	−0.0202	10	0.5122	10	17.0718	
action suggestion		serious deformation transformer must be replaced		obvious deformation maintenance must be started		no fault		
transformer case is		serious deformation and must be replaced						

IET Electr. Power Appl., 2017, Vol. 11, Iss. 3, pp. 412–422

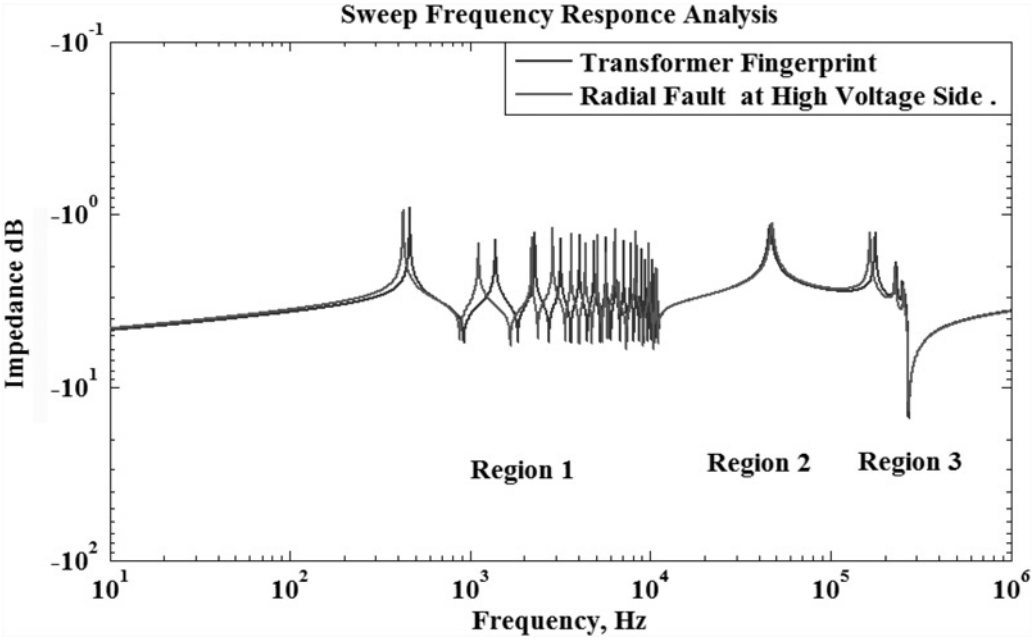

Fig. 6 *SFRA of power transformer at radial fault at HV side*

from 37 to 137 pF). The radial fault simulation is done at disk no. 12-13, to attain variation on a frequency response curve. The SFRA of radial fault at HV side shown in Fig. 6, and the proposed method using CCF algorithm indicators according to three frequency sub-bands are given in Table 9.

5.3.3 Radial fault at LV side: At HV side, this fault is simulated by changing (R_{SL} from 0.75 to 0 Ω), (L_{SL} from 110 mH to 0.0 H), (C_{HL} from 3.3 to 13.3 nF), (C_{SL} from 0.2 to 1.2 nF), and (C_{gL} from 6 to 16 pF). The radial fault simulation is done at disk no. 12-13, in order to attain variation on a frequency response curve. The diagnostic methodology using the CCF technique indicators according to three frequency sub-bands are given in Table 10.

5.4 SC fault between HV and LV sides

In this fault, the insulation material between the HV and LV sides are collapsed or the spacers between them are removed as a result of this fault. This fault is simulated by changing (R_{SL} from 1.2 to 0 Ω), (L_{SL} from 145 μH to 0.0 H), (C_{HL} from 3.3 to 13.3 nF), (C_{SL} from 0.2 to 1.2 nF), (R_{SH} from 0.2 to 0 Ω), (L_{SH} from 110 mH to 0.0 H), and C_{SH} from 2.2 to 12.2 nF). The SFRA of SC between HV and LV shown in Fig. 7, and from Table 11, it can be seen that there is SC fault between HV and LV sides on transformer windings.

5.5 Internal earth faults in power transformer

As it is known the fault current depends upon the value of earthing impedance, the distance between the fault point and the neutral point, the fault current depends upon leakage reactance of the number of winding turns comes across the faulty point and neutral point of the transformer. On the other hand, the leakage reactance of the winding varies in a complex manner with the position of the fault in the winding. It is known that the reactance decreases very rapidly for the fault point approaching the neutral and hence the fault current is highest for the fault near the neutral end. So at this point, the voltage available for fault current is low and at the same time the reactance opposes the fault current is also low, hence, the value of fault current is high. The SFRA of SC-to-ground fault at HV side shown in Fig. 8.

Table 9 Transformer state and comparison of using CCF and CSF techniques at HV radial fault

Analysis factors	Methods	Frequency ranges						Final action for each method
		Low frequency		Medium frequency		High frequency		
		Frequency < 100 kHz		100–600 kHz		Frequency > 600 kHz		
		Ref.	Faulted	Ref.	Faulted	Ref.	Faulted	
Suggestion		Maintenance must be started		Maintenance must be started				
CCF	using CCF technique	1.0000	0.5417	1.0000	0.2054	1.0000	1.0000	serious deformation and transformer must be replaced
action suggestion		obvious deformation maintenance must be started		serious deformation transformer must be replaced		no fault		
variance	previous CSF technique	4.7331×10^{-5}	5.3528×10^{-5}	2.0350×10^{-5}	2.4456×10^{-5}	1.7430×10^{-9}	1.5097×10^{-9}	obvious deformation and maintenance must be started
NCF		1.0000	0.5417	1.0000	0.2054	1.0000	1.0000	
relative factors		10	0.7803	10	0.2299	10	17.1117	
action suggestion		obvious deformation maintenance must be started		obvious deformation maintenance must be started		no fault		
transformer case is		deformation and transformer maintenance must be started						

Table 10 Transformer state and comparison of using CCF and CSF techniques at LV radial fault

Analysis factors	Methods	Frequency ranges						Final action for each method
		Low frequency		Medium frequency		High frequency		
		Frequency < 100 kHz		100–600 kHz		Frequency > 600 kHz		
		Ref.	Faulted	Ref.	Faulted	Ref.	Faulted	
CCF	using CCF	1.0000	0.7908	1.0000	0.6884	1.0000	1.0000	obvious deformation and
action suggestion	technique	slight deformation must be under surveillance		obvious deformation maintenance must be started		no fault		maintenance must be started
variance	previous CSF technique	4.7331×10^{-5}	5.1132×10^{-5}	2.0350×10^{-5}	2.0295×10^{-5}	1.7430×10^{-9}	2.3855×10^{-9}	slight deformation and must be under surveillance
NCF		1.0000	0.7908	1.0000	0.6884	1.0000	1.0000	
relative factors		10	1.5647	10	1.1660	10	17.0928	
action suggestion		slight deformation must be under Surveillance		no fault		no fault		
transformer case is		slight deformation and transformer must be under surveillance						

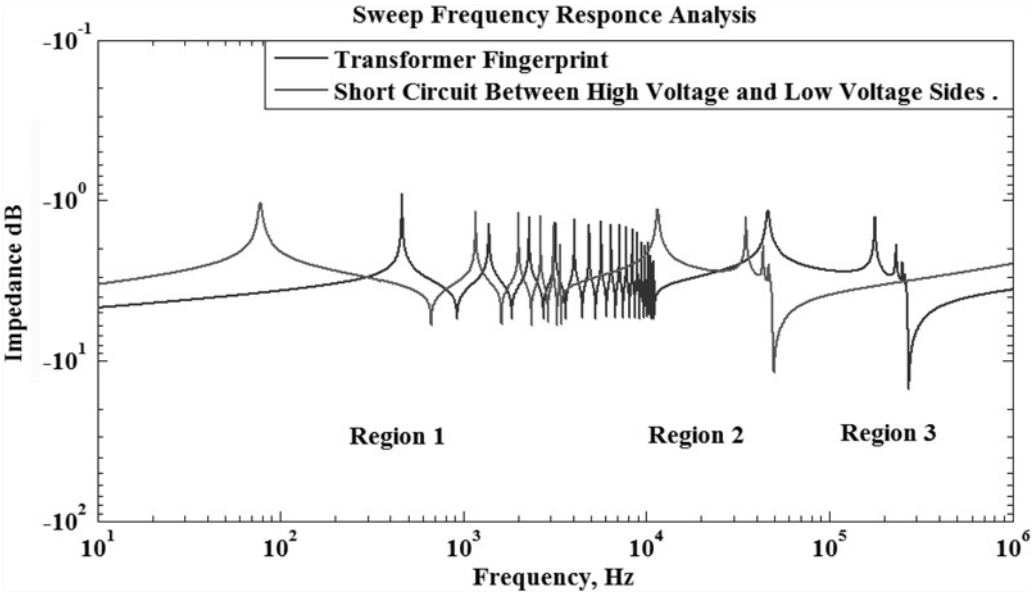

Fig. 7 *SFRA of power transformer at SC between HV and LV sides*

Table 11 Transformer state and comparison of using CCF and CSF techniques at SC fault between HV and LV sides within power transformer

Analysis factors	Methods	Frequency ranges						Final action for each method
		Low frequency		Medium frequency		High frequency		
		Frequency < 100 kHz		100–600 kHz		Frequency > 600 kHz		
		Ref.	Faulted	Ref.	Faulted	Ref.	Faulted	
CCF	using CCF	1.0000	−0.0854	1.0000	−0.2956	1.0000	0.9996	serious deformation and
action suggestion	technique	serious deformation transformer must be replaced		serious deformation transformer must be replaced		no fault		transformer must be replaced
variance	previous CSF technique	4.7331×10^{-5}	8.7121×10^{-5}	2.0350×10^{-5}	2.0540×10^{-7}	1.7430×10^{-9}	1.8165×10^{-7}	serious deformation and transformer must be replaced
NCF		1.0000	−0.0854	1.0000	−0.2956	1.0000	0.9996	
relative factors		10	−0.0820	10	−0.2589	10	7.8365	
action suggestion		serious deformation transformer must be replaced		obvious deformation maintenance must be started		no fault		
transformer case is		serious deformation and must be replaced						

5.5.1 SC-to-ground fault at HV side: Single-line-to-earth fault in which one phase is short-circuited-to-ground is the most commonly occurring of fault types. The shorted simulated by changing (R_{SL} from 1.2 to 0 Ω), (L_{SL} from 145 μH to 0.0 H), (C_{gH} from 37 nF to 37 mF), and (C_{SH} from 2.2 to 2000 nF). Based on the calculations of the diagnostic methodology using the CCF

IET Electr. Power Appl., 2017, Vol. 11, Iss. 3, pp. 412–422

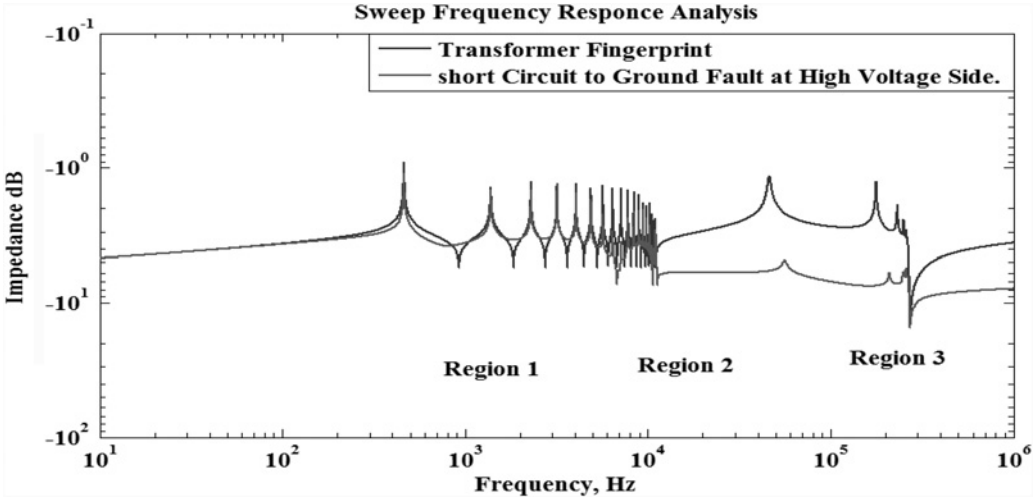

Fig. 8 *SFRA of power transformer at SC-to-ground fault at HV side*

Table 12 Transformer state and comparison of using CCF and CSF techniques at SC-to-ground fault at HV side within power transformer

Analysis factors	Methods	Frequency ranges						Final action for each method
		Low frequency		Medium frequency		High frequency		
		Frequency < 100 kHz		100–600 kHz		Frequency > 600 kHz		
		Ref.	Faulted	Ref.	Faulted	Ref.	Faulted	
CCF	using CCF technique	1.0000	0.6039	1.0000	−0.0106	1.0000	1.0000	obvious deformation and maintenance must be started
action suggestion		obvious deformation maintenance must be started		serious deformation transformer must be replaced		no fault		
variance	previous CSF technique	4.7331×10^{-5}	7.4678×10^{-6}	2.0350×10^{-5}	6.7926×10^{-14}	1.7430×10^{-9}	4.6998×10^{-18}	obvious deformation and maintenance must be started
NCF		1.0000	0.6039	1.0000	−0.0106	1.0000	1.0000	
relative factors		10	0.9261	10	−0.0105	10	13.3130	
action suggestion		obvious deformation maintenance must be started		obvious deformation maintenance must be started		no fault		
transformer case is		deformation and transformer maintenance must be started						

Table 13 Transformer state and comparison of using CCF and CSF techniques at SC-to-ground fault at LV side within power transformer

Analysis factors	Methods	Frequency Ranges						Final action for each method
		Low frequency		Medium frequency		High frequency		
		Frequency < 100 kHz		100–600 kHz		Frequency > 600 kHz		
		Ref.	Faulted	Ref.	Faulted	Ref.	Faulted	
CCF	using CCF technique	1.0000	0.1989	1.0000	0.9201	1.0000	1.0000	serious deformation and transformer must be replaced
action suggestion		serious deformation transformer must be replaced		slight deformation must be under surveillance		no fault		
variance	previous CSF technique	4.7331×10^{-5}	5.6459×10^{-5}	2.0350×10^{-5}	3.4654×10^{-7}	1.7430×10^{-9}	1.4925×10^{-12}	serious deformation and transformer must be replaced
NCF		1.0000	0.1989	1.0000	0.9201	1.0000	1.0000	
relative factors		10	0.2218	10	2.5266	10	10.1279	
action suggestion		serious deformation transformer must be replaced		no fault		no fault		
transformer case is		serious deformation and must be replaced						

technique indicators according to three frequency sub-bands are given in Table 12.

5.5.2 SC-to-ground fault at LV side: At LV side, the short simulation is done by changing (R_{SL} from 0.2 to 0 Ω), (L_{SL} from 110 mH to 0.0 H), (C_{gH} from 6 pF to 6 μF), and C_{SH} from 0.2 to 2 μF) at disk no. (5). Based on the calculations of the diagnostic methodology using the CCF technique indicators according to three frequency sub-bands are given in Table 13.

6 Conclusions

The proposed technique is presented and evaluated for interpreting the results of SFRA measurements. They applied to a number of healthy and faulty transformers as suitable case studies. From the results, the proposed diagnostic methodology using the CCF technique correct identifies the faults inside the transformer. Use CSF technique, which is providing the tools to perform the measurements correctly and interpret the SFRA results to detect any defects in mechanical integrity associated with windings, core and other components of a transformer. The diagnostic methodology using the CCF technique is found to vary significantly and consistently with mechanical displacements taken place in transformers. So these can be considered as the most effective indicator to predict the internal physical condition of the active part of a transformer. The diagnostic methodology using the CCF technique calculation is more objective because it mentions the difference between the measured signal and the result has been divided into certain frequency range. The diagnostic methodology using the CCF technique has been used successfully for the fault identification inactive part of a transformer, but this technique is also applicable to mechanical deformation and damage diagnosis in the transformers. It is important to note that the model used in this study is subject to some assumptions due to neglecting the changes in model parameters of faulty phases. Regrettably these parameters are not easily calculated.

7 References

1 Fairouz, M., Yousof, M., Ekanayake, C., *et al*.: 'Examining the ageing of transformer insulation using FRA and FDS techniques', *IEEE Trans. Dielectr. Electr. Insul.*, 2015, **22**, (2), pp. 1258–1265

2 Bagheri, M., Naderi, M.S., Blackburn, T., *et al*.: 'FRA vs. short circuit impedance measurement in detection of mechanical defects within large power transformer'. Conf. Record of the 2012 IEEE Int. Symp. on Electrical Insulation (ISEI), San Juan, PR, June 2012, pp. 301–305

3 Secue, J.R., Mombello, E.: 'Sweep frequency response analysis (SFRA) for the assessment of winding displacements and deformation in power transformers', *Electr. Power Syst. Res.*, 2008, **78**, (6), pp. 1119–1128

4 Yousof, M.F.M., Ekanayake, C., Saha, T.K.: 'Study of transformer winding deformation by frequency response analysis'. IEEE Power & Energy Society General Meeting, Vancouver, BC, July 2013, pp. 1–5

5 Al Murawwi, E., Barkat, B.: 'A new technique for a better sweep frequency response analysis interpretation'. Conf. Record 2012 IEEE Int. Symp. on Electrical Insulation (ISEI), San Juan, PR, 2012, pp. 366–370

6 Kennedy, G.M., McGrail, A.J., Lapworth, J.A.: 'Using cross-correlation coefficients to: analyze transformer sweep frequency response analysis, (SFRA) traces'. Power Engineering Society Conf. and Exposition in Africa, 2007, Johannesburg, July 2007, pp. 1–6

7 Ghanizadeh, A.J., Gharehpetian, G.B.: 'ANN and cross-correlation based features for discrimination between electrical and mechanical defects and their localization in transformer winding', *IEEE Trans. Dielectr. Electr. Insul.*, 2014, **21**, (5), pp. 2374–2382

8 Al Murawwi, E., Barkat, B., Mardiana, R.: 'Statistical evaluation of a new technique for sweep frequency response analysis'. 2012 IEEE Int. Conf. on Power and Energy (PECon), Kota Kinabalu, December 2012, pp. 741–744

9 Ryder, S.A.: 'Diagnosing transformer faults using frequency response analyses', *IEEE Electr. Insul. Mag.*, 2003, **19**, (2), pp. 16–22

10 Secue, J., Mombello, E., Muela, E.: 'Approach for determining a reliable set of spot frequencies to be used during a sweep frequency response analysis (SFRA) for power transformer diagnosis'. Transmission and Distribution Conf. and Exposition: Latin America, IEEE/PES, 2008, Bogota, August 2008, pp. 1–5

11 De Tommasi, L., Gustavsen, B., Dhaene, T.: 'Robust transfer function identification via an enhanced magnitude vector fitting algorithm', *IET Control Theory Appl.*, 2010, **4**, (7), pp. 1169–1178

12 Chananeò, A., Bouichhida, O., Houassine, H.: 'Investigation of the transformer winding high frequency parameters identification using particle swarm optimization method', *IET Electr. Power Appl.*, 2016, **10**, (9), pp. 923–931

13 Singh, J., Raj, Y., Piush, S., *et al*.: 'Novel method for detection of transformer winding faults using sweep frequency response analysis'. IEEE Power Engineering Society General Meeting, 2007, Tampa, FL, June 2007, pp. 1–9

14 Abu-Siada, A., Islam, S.: 'A Novel online technique to detect power transformer winding faults', *IEEE Trans. Power Deliv.*, 2012, **27**, (2), pp. 849–857

15 Behjat, V., Vahedi, A., Setayeshmehr, A., *et al*.: 'Diagnosing shorted turns on the windings of power transformers based upon online FRA using capacitive and inductive couplings', *IEEE Trans. Power Deliv.*, 2011, **26**, (4), pp. 2123–2133

16 Hashemnia, N., Abu-Siada, A., Islam, S.: 'Impact of axial displacement on power transformer FRA signature'. 2013 IEEE Power & Energy Society General Meeting, Vancouver, BC, July 2013, pp. 1–4

17 Cabral, S.H.L., Mustafa, T.I.A.H., Almagure, H.A.D., *et al*.: 'The role of the distribution transformer in the transference of voltage surges'. Transmission and Distribution Conf. and Exposition: Latin America (T&D-LA), 2010 IEEE/PES, Sao Paulo, 2010, pp. 727–731

18 Abu-Siada, A., Hashemnia, N., Islam, S., *et al*.: 'Understanding power transformer frequency response analysis signatures', *IEEE Electr. Insul. Mag.*, 2013, **29**, (3), pp. 48–56

19 Rahimpour, E., Jabbari, M., Tenbohlen, S.: 'Mathematical comparison methods to assess transfer functions of transformers to detect different types of mechanical faults', *IEEE Trans. Power Deliv.*, 2010, **25**, pp. 2544–2555

20 Mitchell, S.D., Welsh, J.S.: 'Modeling power transformers to support the interpretation of frequency-response analysis', *IEEE Trans. Power Deliv.*, 2011, **26**, pp. 2705–2717

21 Rahimpour, E., Christian, J., Feser, K., *et al*.: 'Transfer function method to diagnose axial displacement and radial deformation of transformer windings', *IEEE Trans. Power Deliv.*, 2003, **18**, pp. 493–505

22 Shintemirov, A., Tang, W.H., Wu, Q.H.: 'Transformer core parameter identification using frequency response analysis', *IEEE Trans. Magn.*, 2010, **46**, pp. 141–149

23 Abeywickrama, N., Serdyuk, Y.V., Gubanski, S.M.: 'High-frequency modeling of power transformers for use in frequency response analysis (FRA)', *IEEE Trans. Power Deliv.*, 2008, **23**, pp. 2042–2049

24 Abu-Siada, A., Hashemnia, N., Islam, S., *et al*.: 'Impact of transformer model parameters variation on FRA signature'. 22nd Australasian, Universities Power Engineering Conf. (AUPEC), 2012 Publications on the IEEE, 26 November 2012, pp. 1–5